厚生労働省科学研究補助金
（医療機器開発推進研究事業（活動領域拡張医療機器開発研究事業））
平成２３年度分担研究報告書

慢性心不全の予後を改善するための非侵襲で安全・安心な無痛性 ICD の実用化臨床試験
植込み型突然死防止装置の開発（分担課題名）

分担研究者　清水　一夫（オリンパス株式会社　医療技術開発本部　医療探索部　部長）

研究要旨：
過去開発してきた植込み型突然死防止装置（ICD）本体の構成（心拍検出回路）を見直し、装置の小型化、低消費電力化を実現した。既存機能として VVI,DDD、CRT（両心室再同期療法）等の最新のペースメーカー機能、頻拍治療、除細動治療の各機能は仕様通りであることを確認した。
心拍検出回路のデジタル化については IC 化を前提に初段の心拍信号増幅器以外デジタル処理の間欠動作により、低消費電力化を実現することを前提に設計を行い、低消費電力化が可能であることを証明した。消費電力としては昨年度のほぼ半分の 60μA を実現した。

A.研究目的

植え込み型除細動器の高性能化を図りつつ、使用する患者の負担を軽減するには、小型化と長寿命化が重要である。

既存 ICD の実現に必要な技術を確立した上で、痛くない除細動機能、及び超小型低消費電力化電子回路の実現を目指す。

弊社分担業務として、植え込み可能な ICD 本体の試作機開発、及び ICD 本体を制御する為のプログラマの開発を行い、機能の確認を行うことを目的とする。

B. 研究方法

B-1.開発手順

昨年度実施した検討をベースに低消費電力化を行うため、デジタルフィルタの検証を行った。まず、検証に使用した機器の構成をベースに回路構成を検討し、シミュレーションにより、回路動作の検証を実施した。
また、過去５年間、厚生労働省科学研究補助金により、植込み型突然死防止装置の開発（Ｈ１５－フィジー００１）を行ってきた成果に基づき、試作実験機の開発を行った。試作実験機の試験は、心拍を模擬した信号発生器により、試験を行い、この試験にて有効性が確認された後、動物実験を行い性能評価を行った。

B-2.倫理面への配慮

動物実験については、九州大学、国立循環器病センター研究所にご協力を頂き、動物実験に関する指針に準拠して行った。

B-3.植込み型突然死防止装置の研究

B-3.1　低消費電力化の研究

従来の ICD 装置の構成を図１に示す。心拍検出および AD 変換、診断の各部分は常時動作す

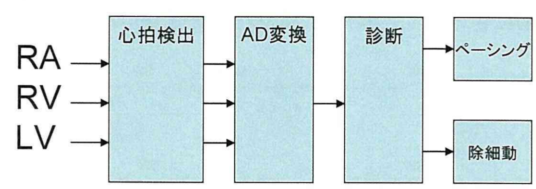

図１　ICD 装置の構成

る必要があり、低消費電力化するには限界がある。そこで、心拍信号のサンプリング間隔に合わせたタイミングでのみ動作するように極力、常時動作するアナログ回路を削減し、デジタル回路による時分割処理を行えるように構成を検討した。(図 2)

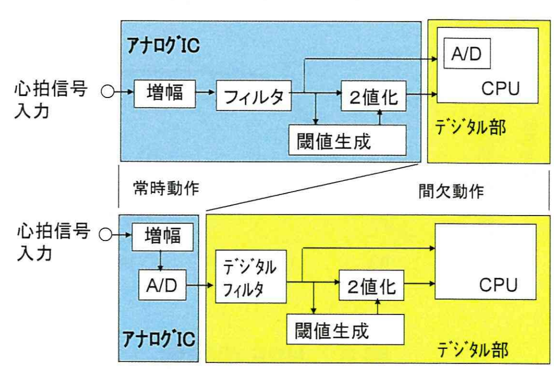

図２　時分割処理を増やした構成

C.研究結果

C-1. デジタルフィルタの研究

従来フィルタリング処理はアナログ回路で実現していたが、今回、デジタルフィルタでの実現を目指した。

図３に心拍信号内の各波形に対するセンシング領域の関係を示す。

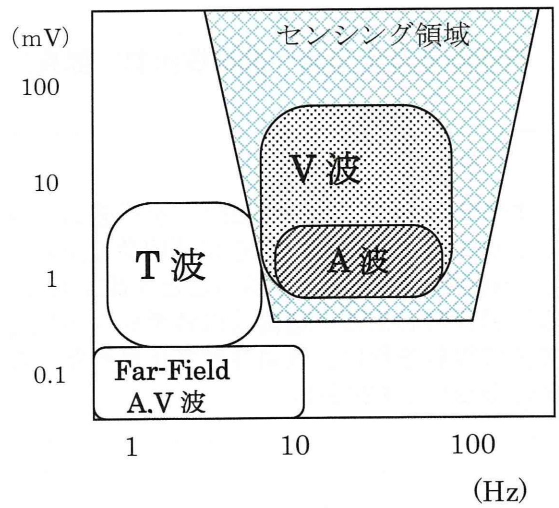

図３　心拍信号内のセンシング領域

図４に今回実現したデジタルフィルタ（HPF）の構成を示す。また、その特性を図５に示す。

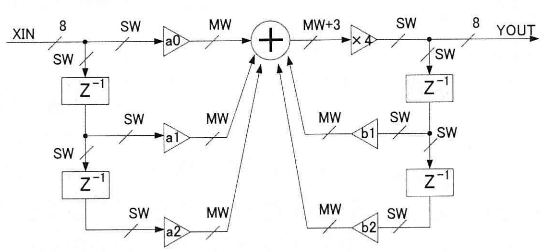

図４　２次 IIR デジタルフィルタ構成

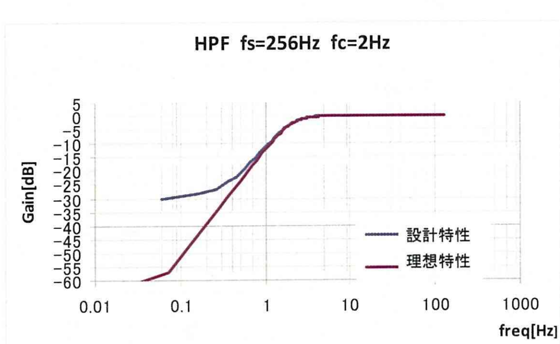

図５　HPF の特性

C-2. 低消費電力化の研究

①消費電力

アナログ回路のみによる心拍検出時の消費電力は 122μA であった。（昨年度の測定値）今回、デジタル化により、図６に示すような間欠動作を行い、低消費電力化を行った。

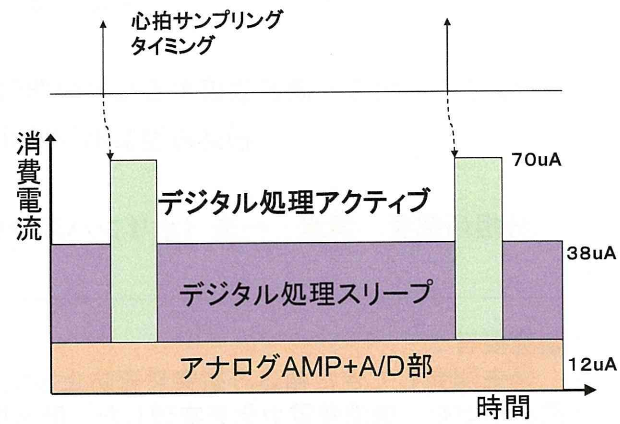

図６　間欠動作による低消費電力化

②心拍検出

ICD 国際規格（EN45502-2-2）における要求仕様に従い試験を実施した。図７に心拍検出用評価回路を示す。

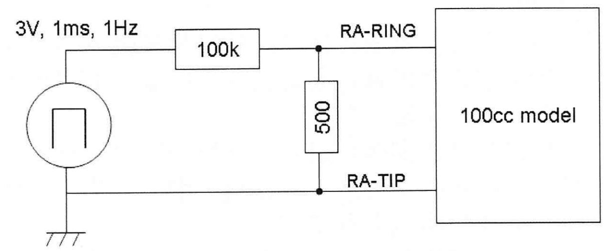

図７　心拍検出評価回路

試験の結果、図８に示すように心拍信号に従い、検出できていることを確認した。

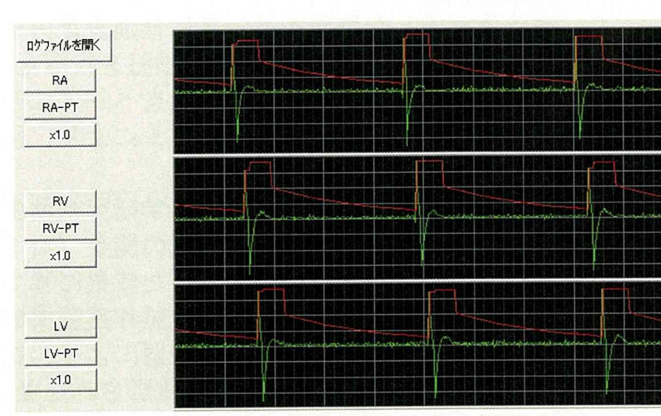

D.考察

昨年度試作した ICD 装置の構成をさらに見直し、検出部のデジタル化により、アナログ検出と比較して、低消費電力化できることを証明し

た。また、デジタル化のメリットとして、デジタルフィルタの特性を複数種類用意したり、オーダーメイドしやすいので、装置の植込み後心拍の検出状況に応じて特性を変えるということも容易になる。さらに、従来アナログ回路で実現していた絶対値回路や ATC 回路もデジタル化により容易に実現することができた。

実際の動作を想定してペーシング率０％と100%における装置寿命を検討した。（表１）

検討条件として、電池容量を２Ah とし、実使用容量１．７５Ah、2 回除細動を行った場合０．２４Ah 消費すると仮定した。

表１　ペーシング動作に伴う本体寿命

ペーシング率		昨年度	本年度
０％	装置寿命	１．６年	３．８年
	消費電流	122μA	50μA
１００％	装置寿命	０．４年	３．１年
	消費電流	470μA	62μA

ペーシング条件：パルス幅 400μs 基本レート 60PPM、ペーシング電圧２．５V、負荷 500Ω

表１から５年以上の寿命を考えると、さらなる低消費電力化を行う必要性を感じる。
このためには常時動作しているアナログ回路の見直し、デジタル回路のリーク電流の削減を検討する必要がある。

E.結論

本年度は検出回路のデジタル化を行い、更なる低消費電力化を検討した。その結果、消費電力も大幅に改善することができた。　しかし、ICD 装置の植込み期間を考えると 50μA 以下にする必要があり、さらなる小型、低消費電力化が必要である。

アルゴリズムの開発並びに動物実験を行うにあたり、九州大学、国立循環器病研究センター研究所、東京大学、東北大学の関係者の皆様より、多大なるご助言、ご協力をいただきました。関係者の皆様に心より感謝申し上げます。

F. 健康危険情報

特になし

G. 研究発表

G-1. 論文
特になし。

G-2. 学会発表
特になし。

G-3. 新聞報道
特になし。

H. 知的所有権の取得状況

特になし。

研究成果の刊行に関する一覧表

書籍

1. Makoto Abe, Telma Keiko Sugai, Makoto Yoshizawa, Kazuo Shimizu, Moe Goto, Masashi Inagaki, Masaru Sugimachi, Kenji Sunagawa. Detection of Life-Thretning Arrhythmias Using Multiple regression Model. In Nano-Biomedical Engineering 2012. Imperial College Press, London. 577-586, 2012.

雑誌

1. Kishi T, Hirooka Y, Katsuki M, Ogawa K, Shinohara K, Isegawa K, Sunagawa K. Exercise Training Causes Sympathoinhibition through Antioxidant Effect in the Rostral Ventrolateral Medulla of Hypertensive Rats. Clin Exp Hypertens. In press, 2012

2. Kishi T, Hirooka Y, Sunagawa K. Sympathoinhibition caused by orally administered telmisartan through inhibition of the AT(1) receptor in the rostral ventrolateral medulla of hypertensive rats. Hypertens Res. In press, 2012

3. Ichiki T, Miyazaki R, Kamiharaguchi A, Hashimoto T, Matsuura H, Kitamoto S, Tokunou T, Sunagawa K. Resveratrol attenuates angiotensin II-induced senescence of vascular smooth muscle cells. Regul Pept. In press, 2012

4. Shinohara K, Hirooka Y, Ogawa K, Kishi T, Yasukawa K, Utsumi H, Sunagawa K. Combination Therapy of Olmesartan and Azelnidipine Inhibits Sympathetic Activity Associated with Reducing Oxidative Stress in the Brain of Hypertensive Rats. Clin Exp Hypertens. In press, 2012

5. Hara M, Tabata K, Suzuki T, Do MK, Mizunoya W, Nakamura M, Nishimura S, Tabata S, Ikeuchi Y, Sunagawa K, Anderson JE, Allen RE, Tatsumi R. Calcium influx through a possible coupling of cation channels impacts skeletal muscle satellite cell activation in response to mechanical stretch. Am J Physiol Cell Physiol. In press, 2012

6. Inoue E, Ichiki T, Takeda K, Matsuura H, Hashimoto T, Ikeda J, Kamiharaguchi A, Sunagawa K. Beraprost sodium, a stable prostacyclin analogue, improves insulin resistance in high-fat diet-induced obese mice. J Endocrinol. 213: 285-291, 2012

7. Miyazaki R, Ichiki T, Hashimoto T, Ikeda J, Kamiharaguchi A, Narabayashi E, Matsuura H, Takeda K, Sunagawa K. Acetylcholinesterase inhibitors attenuate angiogenesis. Clin Sci (Lond). 123: 241-249, 2012.

8. Takemoto M, Mukai Y, Inoue S, Matoba T, Nishizaka M, Ide T, Chishaki A, Sunagawa K. Usefulness of non-contact mapping for radiofrequency catheter ablation of inappropriate sinus tachycardia: new procedural strategy and long-term clinical outcome. Intern Med. 51: 357-362, 2012.

9. Nakagaki T, Hirooka Y, Matsukawa R, Nishihara M, Nakano M, Ito K, Hoka S, Sunagawa K. Activation of mineralocorticoid receptors in the rostral ventrolateral medulla is involved in hypertensive mechanisms in stroke-prone spontaneously hypertensive rats. Hypertens Res. 35: 470-476, 2012.

10. Nishihara M, Hirooka Y, Matsukawa R, Kishi T, Sunagawa K. Oxidative stress in the rostral ventrolateral medulla modulates excitatory and inhibitory inputs in spontaneously hypertensive rats. J Hypertens. 30: 97-106, 2012.

11. Ito K, Hirooka Y, Matsukawa R, Nakano M, Sunagawa K. Decreased brain sigma-1 receptor contributes to the relationship between heart failure and depression. Cardiovasc Res. 93: 33-40, 2012.

12. Miyamoto T, Inagaki M, Takaki H, Kawada T, Shishido T, Kamiya A, Sugimachi M. Adaptation of the respiratory controller contributes to the attenuation of exercise hyperpnea in endurance-trained athletes. Eur J Appl Physiol. 112: 237-251, 2012

13. Makimoto H, Kamakura S, Aihara N, Noda T, Nakajima I, Yokoyama T, Doi A, Kawata H, Yamada Y, Okamura H, Satomi K, Aiba T, Shimizu W. Clinical impact of the number of extrastimuli in

programmed electrical stimulation in patients with Brugada type 1 electrocardiogram. Heart Rhythm. 9: 242-248, 2012

14. Kawata H, Noda T, Yamada Y, Okamura H, Satomi K, Aiba T, Takaki H, Aihara N, Isobe M, Kamakura S, Shimizu W. Effect of sodium-channel blockade on early repolarization in inferior/lateral leads in patients with idiopathic ventricular fibrillation and Brugada syndrome. Heart Rhythm. 9: 77-83, 2012

15. Kawata H, Noda T, Yamada Y, Okamura H, Nakajima H, Kobayashi J, Kamakura S. Abrupt Heart Rate Fallings in a Patient with Biventricular Pacing: Latent Risk for Exacerbation of Heart Failure. Pacing Clin Electrophysiol. 35: e55-e58, 2012

16. Washio T, Okada J, Sugiura S, Hisada T. Approximation for Cooperative Interactions of a Spatially-detailed Cardiac Sarcomere Model. Cellular and Molecular Bioengineering. 5: 113-126, 2012.

17. Hatano A, Okada J, Hisada T, Sugiura S. Critical role of cardiac t-tubule system for the maintenance of contractile function revealed by a 3D integrated model of cardiomyocytes. J Biomech. 45: 815-823. 2012.

18. Sugimachi M, Uemura K, Kawada T, Shishido T, Sunagawa K. Reduction of myocardial oxygen demand by controlling heart rate and hemodynamics simultaneously by novel circulatory model. Conf Proc IEEE Eng Med Biol Soc. 2011:4297-300, 2011.

19. Sakamoto T, Murayama Y, Tanaka A, Sakamoto K, Tobushi T, Saku K, Hosokawa K, Onitsuka K, Fujino T, Sunagawa K. Impact of baroreflex on venous return surface. Conf Proc IEEE Eng Med Biol Soc. 2011: 4295-4296, 2011.

20. Kishi T, Sunagawa K. Experimental 'jet lag' causes sympathoexcitation via oxidative stress through AT1 receptor in the brainstem. Conf Proc IEEE Eng Med Biol Soc. 2011: 1969-1972, 2011.

21. Hosokawa K, Funakoshi K, Tanaka A, Sakamoto T, Onitsuka K, Sakamoto K, Tobushi T, Fujino T, Saku K, Murayama Y, Ide T, Sunagawa K. Artificial baroreflex system restores volume tolerance in the absence of native baroreflex. Conf Proc IEEE Eng Med Biol Soc. 2011: 697-699, 2011.

22. Kawada T, Shimizu S, Sata Y, Kamiya A, Sunagawa K, Sugimachi M. Consideration on step duration to assess open-loop static characteristics of the carotid sinus baroreflex in rats. Conf Proc IEEE Eng Med Biol Soc. 2011: 689-692, 2011.

23. Masuda S, Nakano K, Funakoshi K, Zhao G, Meng W, Kimura S, Matoba T, Miyagawa M, Iwata E, Sunagawa K, Egashira K. Imatinib mesylate-incorporated nanoparticle-eluting stent attenuates in-stent neointimal formation in porcine coronary arteries. J Atheroscler Thromb. 18: 1043-1053, 2011.

24. Matsuura H, Ichiki T, Ikeda J, Takeda K, Miyazaki R, Hashimoto T, Narabayashi E, Kitamoto S, Tokunou T, Sunagawa K. Inhibition of prolyl hydroxylase domain-containing protein downregulates vascular angiotensin II type 1 receptor. Hypertension. 58: 386-393, 2011.

25. Ogawa K, Hirooka Y, Kishi T, Sunagawa K. Brain AT1 receptor activates the sympathetic nervous system through toll-like receptor 4 in mice with heart failure. J Cardiovasc Pharmacol. 58: 543-549, 2011.

26. Matsukawa R, Hirooka Y, Nishihara M, Ito K, Sunagawa K. Neuregulin-1/ErbB signaling in rostral ventrolateral medulla is involved in blood pressure regulation as an antihypertensive system. J Hypertens. 29: 1735-1742, 2011.

27. Kishi T, Hirooka Y, Ogawa K, Konno S, Sunagawa K. Calorie restriction inhibits sympathetic nerve activity via anti-oxidant effect in the rostral ventrolateral medulla of obesity-induced hypertensive rats. Clin Exp Hypertens. 33: 240-245, 2011.

28. Nakagaki T, Hirooka Y, Ito K, Kishi T, Hoka S, Sunagawa K. Role of angiotensin-(1-7) in rostral ventrolateral medulla in blood pressure regulation via sympathetic nerve activity in Wistar-Kyoto and spontaneous hypertensive rats. Clin Exp Hypertens. 33: 223-230, 2011.

29. Hashimoto T, Ichiki T, Ikeda J, Narabayashi E, Matsuura H, Miyazaki R, Inanaga K, Takeda K, Sunagawa K. Inhibition of MDM2 attenuates neointimal hyperplasia via suppression of vascular proliferation and inflammation. Cardiovasc Res. 91: 711-719, 2011.

30. Uemura K, Kawada T, Sunagawa K, Sugimachi M. Peak systolic mitral annulus velocity reflects the status of ventricular-arterial coupling-theoretical and experimental analyses. J Am Soc Echocardiogr. 24: 582-591, 2011.

31. Hirooka Y, Kishi T, Sakai K, Takeshita A, Sunagawa K. Imbalance of central nitric oxide and reactive oxygen species in the regulation of sympathetic activity and neural mechanisms of hypertension. Am J Physiol Regul Integr Comp Physiol. 300: R818-R826, 2011.

32. Chen L, Nakano K, Kimura S, Matoba T, Iwata E, Miyagawa M, Tsujimoto H, Nagaoka K, Kishimoto J, Sunagawa K, Egashira K. Nanoparticle-mediated delivery of pitavastatin into lungs ameliorates the development and induces regression of monocrotaline-induced pulmonary artery hypertension. Hypertension. 57: 343-350, 2011.

33. Fujino T, Nishizaka M, Yufu T, Sunagawa K. A case of multiple focal nodular hyperplasia in the liver which developed after heart transplantation. Intern Med. 50: 43-46, 2011

34. Shimizu S, Akiyama T, Kawada T, Sata Y, Mizuno M, Kamiya A, Shishido T, Inagaki M, Shirai M, Sano S, Sugimachi M. Medetomidine, an α(2)-Adrenergic Agonist, Activates Cardiac Vagal Nerve Through Modulation of Baroreflex Control. Circ J. 76: 152-159, 2011

35. Abe C, Kawada T, Sugimachi M, Morita H. Interaction between vestibulo-cardiovascular reflex and arterial baroreflex during postural change in rats. Appl Physiol. 111: 1614-1621, 2011.

36. Kawada T, Shimizu S, Li M, Kamiya A, Uemura K, Sata Y, Yamamoto H, Sugimachi M. Contrasting effects of moderate vagal stimulation on heart rate and carotid sinus baroreflex-mediated sympathetic arterial pressure regulation in rats. Life Sci. 89: 498-503, 2011

37. Shimizu S, Une D, Shishido T, Kamiya A, Kawada T, Sano S, Sugimachi M. Norwood procedure with non-valved right ventricle to pulmonary artery shunt improves ventricular energetics despite the presence of diastolic regurgitation: a theoretical analysis. J Physiol Sci. 61: 457-465, 2011.

38. Shimizu S, Akiyama T, Kawada T, Sonobe T, Kamiya A, Shishido T, Tokudome T, Hosoda H, Shirai M, Kangawa K, Sugimachi M. Centrally administered ghrelin activates cardiac vagal nerve in anesthetized rabbits. Auton Neurosci. 162: 60-65, 2011.

39. Komamura K, Tatsumi R, Tsujita-Kuroda Y, Onoe T, Matsumoto K, Nakamura T, Miyazaki J, Horio T, Sugimachi M. Cellular injury of cardiomyocytes during hepatocyte growth factor gene transfection with ultrasound-triggered bubble liposome destruction. 2011: 453619, 2011.

40. Kamiya A, Kawada T, Shimizu S, Sugimachi M. Closed-loop spontaneous baroreflex transfer function is inappropriate for system identification of neural arc but partially appropriate for peripheral arc: predictability analysis. J Physiol. 589: 1769-1790, 2011.

41. Mizuno M, Kawada T, Kamiya A, Miyamoto T, Shimizu S, Shishido T, Smith SA, Sugimachi M. Exercise training augments the dynamic heart rate response to vagal but not sympathetic stimulation in rats. Am J Physiol Regul Integr Comp Physiol. 300: R969-R977, 2011.

42. Watanabe H, Nogami A, Ohkubo K, Kawata H, Hayashi Y, Ishikawa T, Makiyama T, Nagao S, Yagihara N, Takehara N, Kawamura Y, Sato A, Okamura K, Hosaka Y, Sato M, Fukae S, Chinushi M, Oda H, Okabe M, Kimura A, Maemura K, Watanabe I, Kamakura S, Horie M, Aizawa Y, Shimizu W, Makita N. Electrocardiographic Characteristics and SCN5A Mutations in Idiopathic Ventricular Fibrillation Associated with Early Repolarization. Circ Arrhythm Electrophysiol. 4: 874-881, 2011.

43. Kurita T, Noda T, Aiba T, Nakajima I, Shimizu W, Motoki K, Yasuoka R, Miyazaki S, Kamakura S. Cardiac resynchronization therapy to prevent life-threatening arrhythmias in patients with congestive heart failure. J Electrocardiol. 44: 736-741, 2011.

44. Makimoto H, Noda T, Kurita T, Nakajima I, Yokoyama T, Doi A, Yamada Y, Okamura H, Satomi K, Aiba T, Shimizu W, Suyama K, Aihara N, Kamakura S. Incessant monomorphic ventricular tachycardia induced by the proarrhythmic effect of amiodarone. Intern Med. 50: 2591-2595, 2011.

45. Ogawa S, Koretsune Y, Yasaka M, Aizawa Y, Atarashi H, Inoue H, Kamakura S, Kumagai K, Mitamura H, Okumura K, Sugi K, Yamashita T. Antithrombotic therapy in atrial fibrillation : evaluation and positioning of new oral anticoagulant agents. Circ J. 75: 1539-1547, 2011.

46. Sekiguchi Y, Tada H, Yoshida K, Seo Y, Li S, Tejima T, Shoda M, Kamakura S, Aonuma K. Significant increase in the incidence of ventricular arrhythmic events after an intrathoracic impedance change measured with a cardiac resynchronization therapy defibrillator. Circ J. 75: 2614-2620, 2011.

47. Yamashita T, Inoue H, Okumura K, Kodama I, Aizawa Y, Atarashi H, Ohe T, Ohtsu H, Kato T, Kamakura S, Kumagai K, Kurachi Y, Koretsune Y, Saikawa T, Sakurai M, Sato T, Sugi K, Nakaya H, Hirai M, Hirayama A, Fukatani M, Mitamura H, Yamazaki T, Watanabe E, Ogawa S. J-RHYTHM II Investigators. Randomized trial of angiotensin II-receptor blocker vs. dihydropiridine calcium channel blocker in the treatment of paroxysmal atrial fibrillation with hypertension (J-RHYTHM II study). Europace. 13: 473-479, 2011.

48. Okada J, Washio T, Maehara A, Momomura S, Sugiura S, Hisada T Transmural and apicobasal gradients in repolarization contribute to T-wave genesis in human surface ECG. Am J Physiol Heart Circ Physiol. 301: H200-H208, 2011.

49. Hatano A, Okada J, Washio T, Hisada T, Sugiura S. A three-dimensional simulation model of cardiomyocyte integrating excitation-contraction coupling and metabolism. Biophys J. 101: 2601-2610, 2011.

50. Norihiro Sugita, Makoto Yoshizawa, Akira Tanaka, Makoto Abe, Noriyasu Homma, Shigeru Chiba, Tomoyuki Yambe, Shin-ichi Nitta. Evaluation of temporal relationship between a physiological index and a subjective score using average mutual information. Displays. 32: 201-208, 2011.

51. 阿部　誠，吉澤　誠，杉田　典大，田中　明，本間　経康，山家　智之，仁田　新一：容積脈波の独立成分分析による圧受容器反射機能の評価　電気学会論文誌 C　131: 1540-1546, 2011.

52. 阿部　誠, テルマ　ケイコ　スガイ, 吉澤　誠, 本間　経康, 杉田　典大, 清水　一夫, 後藤　萌, 稲垣　正司, 杉町　勝, 砂川　賢二：植込み型除細動器用致死性不整脈検出アルゴリズムの高速・高精度化　生体医工学　49:932-938, 2011.

NANO-BIOMEDICAL ENGINEERING 2012

Proceedings of the Tohoku University Global Centre of Excellence Programme

Global Nano-Biomedical Engineering Education and Research Network Centre

Sakura Hall, Tohoku University,
Sendai Japan, 5 – 6 March 2012

Editor

Takami Yamaguchi, MD PhD

School of Biomedical Engineering, Tohoku University

Published by

Imperial College Press
57 Shelton Street
Covent Garden
London WC2H 9HE

Distributed by

World Scientific Publishing Co. Pte. Ltd.
5 Toh Tuck Link, Singapore 596224
USA office: 27 Warren Street, Suite 401-402, Hackensack, NJ 07601
UK office: 57 Shelton Street, Covent Garden, London WC2H 9HE

British Library Cataloguing-in-Publication Data
A catalogue record for this book is available from the British Library.

NANO-BIOMEDICAL ENGINEERING 2012
Proceedings of the Tohoku University Global Centre of Excellence Programme

ISBN-13 978-1-84816-905-0
ISBN-10 1-84816-905-1

Printed in Singapore by Mainland Press Pte Ltd.

DETECTION OF LIFE-THREATENING ARRHYTHMIAS USING MULTIPLE REGRESSION MODEL

MAKOTO ABE[1)*], TELMA KEIKO SUGAI[2)], MAKOTO YOSHIZAWA[3)†], KAZUO SHIMIZU[4)], MOE GOTO[4)], MASASHI INAGAKI[5)], MASARU SUGIMACHI[5)], KENJI SUNAGAWA[6)]

1) Graduate School of Engineering, Tohoku University, 6-3, Aoba, Aramaki, Aoba-ku, Sendai, Miyagi 980-8578, Japan

2) Graduate School of Biomedical Engineering, Tohoku University, 6-3, Aoba, Aramaki, Aoba-ku, Sendai, Miyagi 980-8578, Japan

3) Research Division on Advanced Information Technology, Cyberscience Center, Tohoku University, 6-3, Aoba, Aramaki, Aoba-ku, Sendai, Miyagi 980-8578, Japan

4) Olympus Corporation, 2-3, Kuboyama-cho, Hachioji, Tokyo 192-8512, Japan

5) National Cerebral and Cardiovascular Center Research Institute, 5-7-1, Fujishirodai, Suita, Osaka 565-8565, Japan

6) Graduate School of Medicine, Kyushu University, 3-1-1, Maidashi, Higashi-ku, Fukuoka, Fukuoka 812-8582, Japan

The implantable cardioverter-defibrillator is an effective therapeutic device for saving patients with cardiac diseases from death caused by life-threatening arrhythmias such as ventricular tachycardia and ventricular fibrillation. It is important to prevent the recurrence and treat these arrhythmias early and to accurately distinguish between a normal sinus rhythm, ventricular tachycardia, ventricular fibrillation, and supraventricular tachycardia. Therefore, in this study, we have proposed a multiple regression model based on information extracted from simultaneous intracardiac electrocardiograms in order to identify episodes of supraventricular tachycardia, ventricular tachycardia, and ventricular fibrillation. From the experimental results, we confirmed that life-threatening arrhythmias can be detected on the basis of indices obtained from simultaneous intracardiac electrocardiograms.

Keywords: implantable cardioverter-defibrillator, arrhythmia, multiple regression model

1. Introduction

The number of victims of sudden cardiac death is estimated to be ~70,000 per year in Japan and it is increasing continuously. A sudden cardiac death is

---

* Makoto Abe was a Tohoku University Global COE Research Assistant (2007-2008).
† Makoto Yoshizawa is a Tohoku University Global COE Member.

directly caused by life-threatening cardiac arrhythmia such as ventricular tachycardia (VT) and ventricular fibrillation (VF). The survival rates for these arrhythmias decrease by 7–10% per minute; therefore, it is important to treat these arrhythmias early [1]. The implantable cardioverter-defibrillator (ICD) is an effective therapeutic device for saving patients with cardiac diseases from death caused by life-threatening arrhythmia. However, the traditional algorithms used in ICD for detecting VF and VT are based almost only on the information for the cardiac period [2], thus making it difficult to accurately distinguish between a normal sinus rhythm, VT, VF, and supraventricular tachycardia (SVT).

Furthermore, the incidence of inappropriate ICD treatment has not reduced. A recent study found inappropriate VT detection in 14% of patients treated for secondary sudden cardiac death prevention and in 30% of patients treated for primary prevention [3]. Another study reported positive detection of VTs using modern, optimized ICD detection algorithms in only 60–70% of patients with spontaneous tachycardias [4]. These detection errors are related to different causes; for example, ventricular oversensing causes inappropriate therapy in up to 25% of patients [3].

In order to treat VF or VT accurately, it is necessary to improve the classification algorithms that can distinguish shockable cardiac rhythms from nonshockable cardiac rhythms. In addition, these algorithms should detect arrhythmias as fast as possible.

In this study, we have proposed a method based on information extracted from intracardiac electrocardiograms (IECGs) to identify episodes of SVT, VT, and VF. IECGs were measured from the left ventricle ($IECG_{LV}$), right ventricle ($IECG_{RV}$), and right atrium ($IECG_{RA}$). The arrhythmias were classified by inputting 14 input indices obtained from these IECGs to a multiple regression model. It was possible to identify life-threatening arrhythmias within a short time with a relatively high accuracy. The proposed method was validated by performing an animal experiment.

2. Methods

2.1. *Data Description and Preprocessing*

In this study, experimental data were obtained from five dogs (*in vivo*) in an acute experiment. IECGs were measured using leads from the left and right ventricles and the right atrium. These data were sampled at 200 Hz or 1 kHz and then resampled at 250 Hz. In addition, owing to the difficulty in measuring spontaneous arrhythmia, SVT, VT, and VF were simulated as follows. SVT was simulated by right atrial pacing. VT was simulated by right or left ventricular pacing, and VF was induced by applying electrical stimuli after the R-wave of the surface electrocardiogram. The data also included one spontaneous VF episode.

First, a bandpass filter (0.8–40 Hz) was applied to the IECG signals in order to remove the noise component. After filtering, the data were analyzed using a moving data window with a length of 1.0 s and shift of 0.2 s, as shown in Fig. 1.

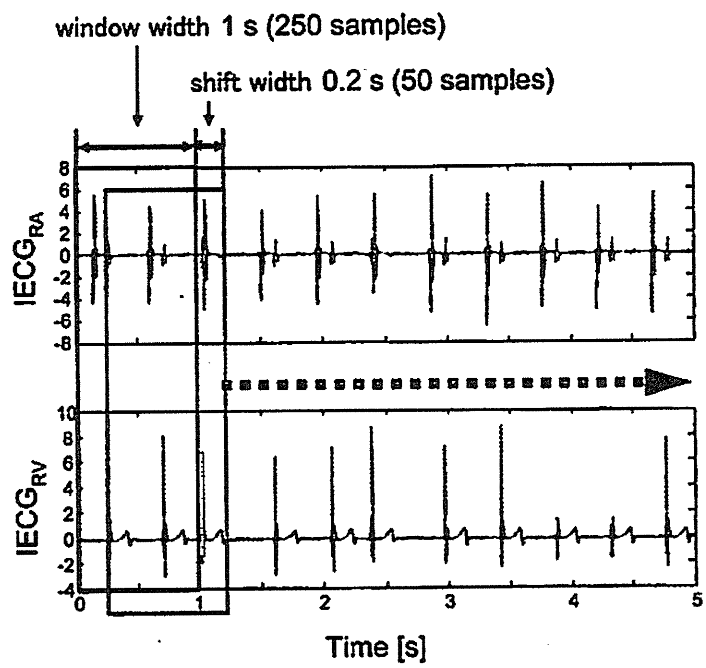

Figure 1. Data acquisition using 1-s-long window with 0.2-s shift

2.2. *Classification*

First, k is defined as the discrete time, which is increased by shifting window in every 0.2 s. Our multiple regression method is described as follows.

1. Let $x_1(k), x_2(k), ..., x_m(k)$ be m feature variables extracted from IECGs signal at the kth window. Define a feature vector $\boldsymbol{x}(k)$ as $\boldsymbol{x}(k) = [x_1(k), x_2(k), ..., x_m(k)]^T$.
2. Cardiac rhythms, SR, SVT, VT, and VF, are numbered from $i = 1$ to $i = 4$. The result of detection is described as follows:

$$y_i(k) = \begin{cases} 1 \text{ (if the sample belongs to the rhythm } i) \\ 0 \text{ (otherwise)} \end{cases} \quad (1)$$

Define the result of a detection vector $\boldsymbol{y}(k)$ as $\boldsymbol{y}(k) = [y_1(k), y_2(k), ..., y_4(k)]^T$.

3. Assume that the feature vector $x(k)$ is given as explanatory variable and $y(k)$ given as objective variable, a multiple regression model is described as follows:

$$y(k) = Ax(k) + e(k), \tag{2}$$

where $4 \times m$ matrix A is a regression coefficients matrix and 4×1 vector $e(k)$ is a disturbance term.

In this study, m was set to 14 and the number of windows K was set to 400 experimentally. The matrix A was calculated by the least-squares method using Equation (2). A model for each rhythm according to Equation (1) was estimated by the training dataset. The same training dataset was used for the identification of the four models of rhythms.

2.3. *Indices Based on IECGs*

2.3.1. *Histogram distribution*

In order to evaluate the index of independence between the atrial ECG and the ventricular ECG, the simultaneous frequency distribution between pairs of IECGs is expressed by five times five bins, and the Pearson's χ^2 statistic was calculated from the distribution [5]. In addition, the dispersion of the histogram was calculated as the standard deviation (σ) of the counts in each bin of the histogram.

In this study, χ^2 statistic and σ were calculated from between $IECG_{LV}$ and $IECG_{RV}$ and from between $IECG_{RA}$ and $IECG_{RV}$, which gave us the four indices extracted from the histograms.

2.3.2. *Cardiac periods*

The periods (R-R intervals) were the only indices extracted from single IECGs. In general, the cardiac period is obtained from the R-R interval using an R-wave detection method. In this study, a method with an auto-correlation function was proposed to detect the R-wave even though IECGs included much noise. The period was approximated to the time of the first peak of the auto-correlation function of each IECG in the moving 1s- window.

The cardiac periods $Period_{LV}$, $Period_{RV}$, and $Period_{RA}$ were obtained from $IECG_{LV}$, $IECG_{RA}$, and $IECG_{RV}$, respectively. In addition, we calculated the ratio between $Period_{LV}$ and $Period_{RV}$ and between $Period_{RA}$ and $Period_{RV}$.

2.3.3. *Relative delays*

The relative delay was calculated from the cross-correlation function between two IECG signals. The relative delay from $IECG_{RA}$ to $IECG_{RV}$ and that from $IECG_{RA}$ to $IECG_{RV}$ were calculated.

The relative delays and the relative periods of IECGs reflect the atrioventricular conduction. If two IECGs synchronize, the delay is almost constant. While, if two IECGs are in condition of asynchronous, the delay is inconstant. The constancy of the R-P interval is known to be a reliable diagnostic criterion for VT.

2.3.4. *Complex plain based on simultaneous distribution of IECGs*

Finally, the main angle of the distribution of two IECGs and the length of the depolarization were considered.

In order to facilitate the calculations, a complex number Z was defined as follows:

$$Z = IECG_{\mathrm{RV}} + i \cdot IECG_{\mathrm{LV}}, \tag{3}$$

where i is the imaginary unit. The first and third quartile points of the angle of Z were used to represent the angle of the distribution. The main angle was bigger in VT events (~80°) than in SVTs (~50°).

The length of the depolarization was approximated to the count of point of

$$|Z| > 0.05 \cdot \max_{1\,\mathrm{s\ window}} |Z|. \tag{4}$$

In VF, the length was almost 250 (window length) because depolarization was produced during most of the cardiac cycle. On the other hand, the length was smaller in SR, when the R-R intervals are bigger, and intermediate in the tachycardia.

2.3.5. *Validation*

In order to assess the validity of the proposed method, n (from 100 to 600 every 100) windows were randomly selected for the training set and the remaining 5221 windows were used in the test set. In addition, the validation process was repeated 100 times so as to evaluate the robustness of the method.

All the indices were normalized in the training process. The same normalization coefficients were used to normalize the test set.

For the evaluation of the classifier, the area under the receiver operating characteristic (*ROCA*), the sensitivity, and the specificity were used. The closer the *ROCA* value of the classifier is to 1, the more effective it is. The receiver operating characteristic (ROC) represents the sensitivity versus (1 - specificity) for a binary classifier system with a varying discrimination threshold. Sensitivity and specificity are defined in Eqs. (5) and (6), respectively.

$$Sensitivity = \frac{TP}{TP + FN} \tag{5}$$

$$Specificity = \frac{TN}{TN + FP}, \tag{6}$$

where TP is the number of true positives, FN is the number of false negatives, TN is the number of true negatives, and FP is the number of false positives.

3. Results

In this study, even though the classification was performed with four models, one for each rhythm, the sensitivity and specificity were calculated by considering the SVT and SR as the same class, because in both cases, the ICD was not activated.

Figures 2–4 show examples of measured signals and the corresponding output of the classifier obtained using the method described in section 2.2, before and at the beginning of different arrhythmias.

The validation results of classification by the linear regression method are listed in Table 1. Figure 5 shows the *ROCA*s of binary classification for each of the four models.

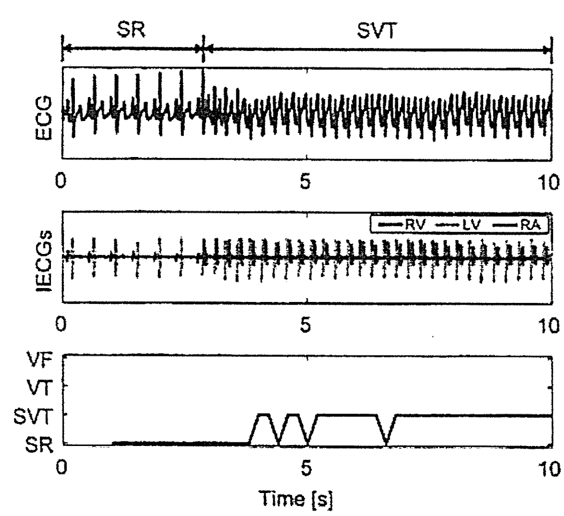

Figure 2. Example of surface ECG (top), IECGs (middle), and corresponding classifier output (bottom) at beginning of SVT episode.

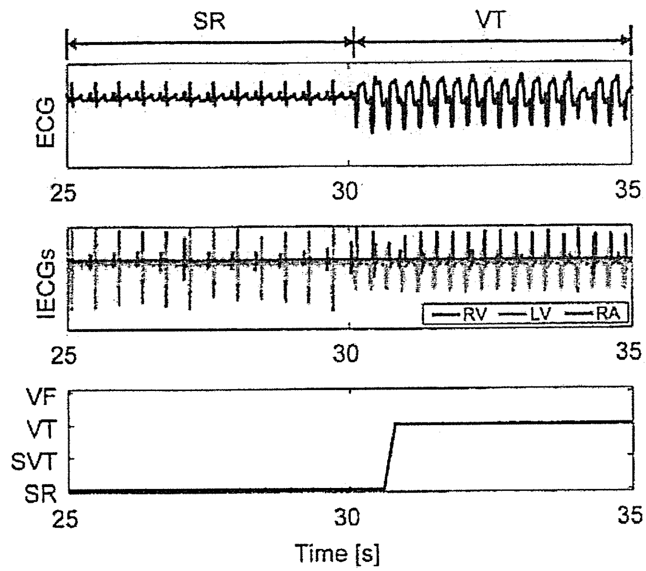

Figure 3. Example of surface ECG (top), IECGs (middle), and corresponding classifier output (bottom) at beginning of VT episode.

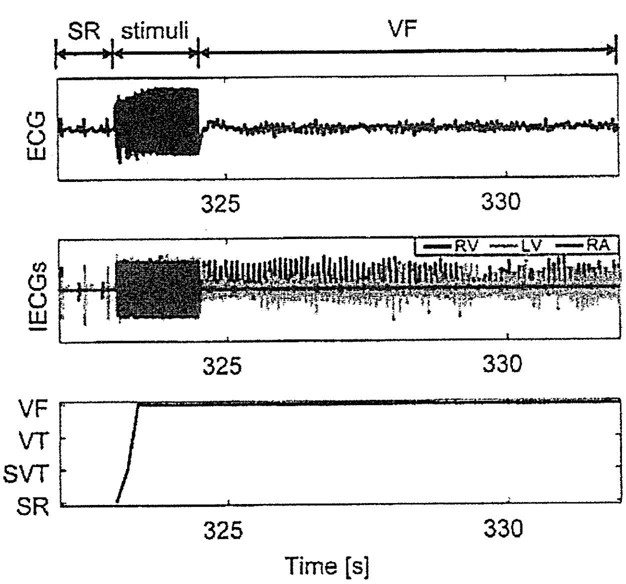

Figure 4. Example of surface ECG (top), IECGs (middle), and corresponding classifier output (bottom) at beginning of VF episode.

Table 1. Validation results for specificity and sensitivity of detection of each rhythm

	Specificity (%)	*Sensitivity* (%)
SR or SVT	98.3	96.8
VT	99.0	73.7
VF	97.4	97.4

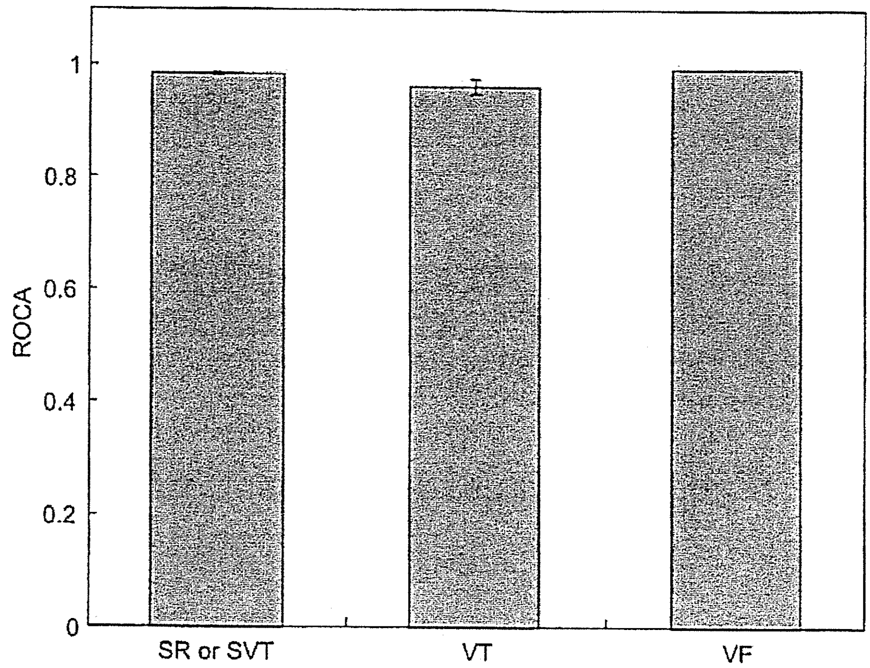

Figure 5. *ROCA* of model of each rhythm obtained from randomly selected training sets (the bars represent the mean value and the error bars represent the standard variation of *ROCA*).

4. Discussion

The results show that the proposed method could classify the cardiac rhythms SR, SVT, VT, and VF with high accuracy. In particular, Fig. 5 shows that the *ROCA* using the evaluated model was >0.94.

The use of the χ^2 statistics and σ was evaluated in a previous phase of this study [5]. These two indices enable early detection of arrhythmias; however, the accuracy of detection using only these indices is lower than that of other conventional methods, which motivated us to use additional indices for detection. Another limitation of the previous study was that only the ventricular IECGs were used, and therefore, it was difficult to distinguish between SVT and VT. Using the same dataset as in the present study, the classification proposed in the previous study resulted in the sensitivity and the specificity of, respectively, 82.7% and 80.3% for SVT or SR, 66.5% and 85.1% for VT, and 79.9% and 99.4% for VF. Most of the misclassification was SVT being classified as VT. Thus, it should be noted that this would lead to unnecessary activation of the ICD. On the other hand, in the present study, sensitivity of the detection of life-threatening arrhythmias was >73.7% and specificity was >96.8%. The low sensitivity in the detection of VTs is mostly due to the misclassification of VTs as SR or SVT.

The delay in the detection was ~1.2 s for SVTs, 1.6 s for VTs, and 1 s for VFs. Because VFs were preceded by an electrical stimulus, the delay in

References

1. American Heart Association, 2005 American Heart Association Guidelines for cardiopulmonary resuscitation and emergency cardiovascular care. *Circulation* **112**, IV-35–IV-46 (2005).
2. A. Przybylskia, R. Baranowskia, J. J. Zebrowskib and H. Szweda, Verification of implantable cardioverter defibrillator (ICD) interventions by nonlinear analysis of heart rate variability—preliminary results. *Europace* **6**, 617–624 (2004).
3. C. W. Israel, How to avoid inappropriate therapy. *Current Opinion in Cardiology* **23**, 65–71 (2008).
4. J. Gillberg, Detection of cardiac tachyarrhythmias in implantable devices. *Journal of Electrocardiology* **40**, S123–S128 (2007).
5. H. Kinoshita, M. Yoshizawa, M. Inagaki, K. Uemura, M. Sugimachi and K. Sunagawa, Development of an algorithm for detection of fatal cardiac arrhythmia for implantable cardioverter-defibrillator using a self-organizing map. In *Proceedings of the 28th IEEE EMBS Annual International Conference*, New York, 4370–4373 (2006).

detection could be evaluated in only one episode. These results indicate that life-threatening arrhythmias could be detected early by using the classification based on the proposed method. This early detection is mainly attributed to the short length of the window (1s length) used to extract the selected indices.

The validation using the training set, which was randomly selected, does not guarantee a uniform distribution of each rhythm in the training set, especially of rhythms with few available data (*e.g.*, VT). This fact explains the high standard deviation in the *ROCA*s of the model of some rhythms. Furthermore, the distribution of each rhythm is not uniform in the validation set.

The main limitation of this study is that these results were obtained from a limited dataset. The algorithm should be evaluated using more data obtained under different conditions. Moreover, it is important to consider the computational and memory cost that each additional index presents.

5. Conclusion

We proposed a new algorithm for the detection of arrhythmias using ICDs. Each cardiac rhythm was classified by a multiple regression model using the indices obtained from IECG signals as inputs. The following indices were used: χ^2 statistics and standard deviation σ extracted from 2D histograms, period of each IECG and their relative ratio, delay between pairs of IECGs, main angle of distribution of two IECGs, and length of depolarization.

In the proposed method, four groups of cardiac rhythms were considered: SR, SVT, VT, and VF. The relative delay in the detection of life-threatening arrhythmias considerably affects the efficiency of the treatment. In this study, changes in the rhythms could be detected rapidly using short windows while maintaining the good performance of the classifier. The proposed method showed a sensitivity of at least 76.0% and specificity of at least 96.8% for a dataset including the data for five subjects. Thus, information from pairs of simultaneous electrocardiograms enables fast and accurate detection of arrhythmias.

Acknowledgments

Makoto Abe gratefully acknowledges the support of the Tohoku University Global COE Program: "Global Nano-Biomedical Engineering Network Centre."